Biofilm 4 (2022) 100093

Contents lists available at ScienceDirect

Biofilm

journal homepage: www.sciencedirect.com/journal/biofilm

Functional analysis of intergenic regulatory regions of genes encoding surface adhesins in *Staphylococcus aureus* isolates from periprosthetic joint infections

Liliana Morales-Laverde [a], Margarita Trobos [b], Maite Echeverz [a], Cristina Solano [a], Iñigo Lasa [a,*]

[a] *Laboratory of Microbial Pathogenesis. Navarrabiomed, Hospital Universitario de Navarra (HUN), Universidad Pública de Navarra (UPNA), IdiSNA, Pamplona, 31008, Spain*
[b] *Department of Biomaterials, Institute of Clinical Sciences, Sahlgrenska Academy, University of Gothenburg. Gothenburg, Sweden*

A R T I C L E I N F O

Keywords:
Periprosthetic joint infection
LPXTG proteins
SNPs
Intergenic regions
Staphylococcus aureus
Biofilm

A B S T R A C T

Staphylococcus aureus is a leading cause of prosthetic joint infections (PJI). Surface adhesins play an important role in the primary attachment to plasma proteins that coat the surface of prosthetic devices after implantation. Previous efforts to identify a genetic component of the bacterium that confers an enhanced capacity to cause PJI have focused on gene content, kmers, or single-nucleotide polymorphisms (SNPs) in coding sequences. Here, using a collection of *S. aureus* strains isolated from PJI and wounds, we investigated whether genetic variations in the regulatory region of genes encoding surface adhesins lead to differences in their expression levels and modulate the capacity of *S. aureus* to colonize implanted prosthetic devices. The data revealed that *S. aureus* isolates from the same clonal complex (CC) contain a specific pattern of SNPs in the regulatory region of genes encoding surface adhesins. As a consequence, each clonal lineage shows a specific profile of surface proteins expression. Co-infection experiments with representative isolates of the most prevalent CCs demonstrated that some lineages have a higher capacity to colonize implanted catheters in a murine infection model, which correlated with a greater ability to form a biofilm on coated surfaces with plasma proteins. Together, results indicate that differences in the expression level of surface adhesins may modulate the propensity of *S. aureus* strains to cause PJI. Given the high conservation of surface proteins among staphylococci, our work lays the framework for investigating how diversification at intergenic regulatory regions affects the capacity of *S. aureus* to colonize the surface of medical implants.

1. Introduction

A major challenge that microbiologists face in the post-genomic era is to identify those differences in bacterial genomes most likely related to phenotypic abilities to cause disease. Intraspecies variation in bacterial genomes occurs through differences in genome content (gene gain or loss) and point mutations caused by punctual insertions, deletions, and single nucleotide polymorphisms (SNPs) [1–4]. Acquisition of new genes can promote more rapid adaptation to new environments than the accumulation of spontaneous mutations because they derive from strains already adapted to a specific niche [5]. The effect of point mutations on bacterial adaptation depends on whether mutations occur in protein-coding sequences or intergenic regions (IGRs). SNPs in protein-coding sequences can lead to frameshifts that interrupt protein translation or changes in the amino acid sequence that enhance or reduce the protein activity, and consequently, bacterial fitness to a particular niche [6]. When point mutations occur at IGRs, they may influence the expression of neighbouring genes or regulatory non-coding RNA molecules. In this case, the causal link between the SNPs and the host-adaptive trait is less recognizable, and functional validation assays are needed to support the relationship between the genotype and the phenotype [7,8].

Staphylococcus aureus is one of the most important Gram-positive bacterial pathogens that can form biofilms on medical devices such as catheters, valves and prostheses [9,10]. *S. aureus* from skin and mucous membranes from the patient or health care personnel can adhere to the surface of the implant via nonspecific interactions based on the physicochemical properties of the cell envelope or through specific binding

* Corresponding author.
E-mail address: ilasa@unavarra.es (I. Lasa).

https://doi.org/10.1016/j.bioflm.2022.100093
Received 18 August 2022; Received in revised form 31 October 2022; Accepted 7 November 2022
Available online 8 November 2022

between adhesins present on the cell surface and proteins of the host plasma that coat the surface of the implanted material soon after insertion [11,12]. Bacterial attachment is followed by bacterial division and synthesis of a matrix to form multicellular communities that protect bacteria from the immune system and the effects of antibiotics [13,14]. As a consequence, staphylococcal biofilm-associated infections are difficult to eradicate and, in most cases, contaminated implants need to be removed to cure the infection [15,16].

S. aureus produces several adhesins that promote initial attachment and cell-to-cell interactions during biofilm formation [17]. Proteinaceous adhesins include cell wall-anchored (CWA) proteins and non-covalently associated surface proteins [17–19]. The major group in the CWA proteins corresponds to the MSCRAMM (microbial surface components recognizing adhesive matrix molecules) family of proteins [20] and includes, among others, the clumping factor (Clf)-serine aspartate repeat (Sdr) family of proteins, the bone sialoprotein-binding protein (Bbp); the fibronectin-binding proteins (FnBPs); and the collagen-binding protein (Cna). Non-covalently associated surface adhesins include the SERAM (secretable expanded repertoire adhesive molecules) family with the extracellular fibrinogen binding protein (Efb), the extracellular matrix binding protein (Emp), and the extracellular adherence protein (Eap) as the most representative members [17,21]. Although the main function of surface adhesins is to promote adhesion to host extracellular matrix proteins, they can also contribute to other functions such as immune system evasion [10]. Another characteristic of surface adhesins is that they are functionally redundant and different surface adhesins can recognize the same ligand. This functional redundancy implies that the absence of an adhesin may be partially compensated by others [22]. The sequence of surface adhesins is under constant selective pressure to aid in the evasion of host defences. Sequence analysis of FnBPA and FnBPB of *S. aureus* strains isolated from patients with endocarditis showed polymorphisms in the amino acid sequence that might have been selected to increase the binding affinity to fibronectin (Fn) [23,24]. The level of surface adhesin expression can also vary between clinical *S. aureus* isolates [11], and within the same strain grown under different environmental conditions [11,25]. For instance, it is known that under iron-limiting conditions, *S. aureus* induces the expression of Isd proteins, as well as the secreted Eap and Emp proteins [26]. However, how important is genetic diversification of surface adhesins expression within *S. aureus* lineages that colonize medical implants in niche specialization remains unknown.

In this study, we investigated whether *S. aureus* clinical isolates might differ in their capacity to cause PJI depending on the presence of SNPs in the IGRs upstream of the translation start site of genes encoding surface adhesins. The results revealed that SNPs heterogeneity results in a specific pattern of surface adhesins expression in each genetic lineage that might confer a competitive advantage in the colonization of prostheses.

2. Materials and methods

2.1. Bacterial strains, plasmids, oligonucleotides, and culture conditions

Bacterial strains, plasmids, and oligonucleotides are listed in Supplementary tables S1, S2 and S3. The forty-five PJI *S. aureus* strains were previously isolated at Sahlgrenska Hospital (Sweden) from PJI of the hip or knee [27,28]. Twenty-six strains from wound infections, isolated between 1966 and 2010, were obtained from the Culture Collection University of Gothenburg (CCUG) [29,30]. *Escherichia coli* and *S. aureus* were grown in Luria-Bertani medium (LB; Conda-Pronadisa, Madrid, Spain) and Trypticase soy broth (TSB; Conda-Pronadisa, Madrid, Spain) at 37 °C. Bacteriological agar was used as a gelling agent (VWR, Radnor, PA, USA). When required, growth media were supplemented with antibiotics at the following concentrations: erythromycin (Ery), 10 μg/mL or 2.5 μg/mL; ampicillin (Amp), 100 μg/mL.

2.2. DNA manipulations

Unless specified otherwise, all the experiments were conducted in accordance with standard practices and manufacturer's instructions. Restriction enzymes (FastDigest), DNA polymerase (Phusion), and the quick DNA ligation kit from Thermo Scientific (Waltham, MA, USA) were used for cloning research. A Macherey-Nagel plasmid purification kit (Allentown, PA, USA) was used to purify the plasmids before they were electroporated into *Escherichia coli* (1 mm cuvette; 200 Ω, 25 μF, 1250 V) or *S. aureus* (1 mm cuvette; 100 Ω, 25 μF, 1250 V) with a Gene Pulser X-Cell electroporator. Gene Competent cells were prepared as previously stated [31]. The oligonucleotides were synthesized by STABVIDA Lda (Caparica, Portugal), and sanger sequencing was used to confirm the sequences of all generated plasmids.

2.3. Whole-genome sequencing and genomic analysis

Whole genome sequencing of PJI and wound isolates was previously performed [27,29]. The Sequence Read Archives (SRAs) including comprehensive data on the strains were submitted to the National Center for Biotechnology Information (NCBI) and given the BioProject accession number PRJNA765573.

Nodes containing the locus of twenty-three genes encoding adhesins, were localized in each strain using the blastn tool from the NCBI website. Analysis of the SNPs and comparison between the strains was performed with SnapGene v5.3.3. All sequences were aligned and compared against the *S. aureus* MW2 genome (GenBank accession number NC_003923). Genetic analysis was focused on the promoter region of adhesin-encoding genes *fnbA, clfA, clfB, sdrC, spa, sasC, sasE* (*isdA*), *sasF, sasH* (*adsA*), *sasI* (*isdH*), *sasJ* (*isdB*), *eap, emp, vw*b and *efb*, which were present in all strains. For PJI isolates, sequence typing (ST) was previously performed [27,28]. We used the MLST 2.0 tool (https://cge.cbs.dtu.dk/services/MLST/) and the Bacterial Isolate Genome Sequence Database (BIGSdb) (https://pubmlst.org/) to group the isolates from wounds.

2.4. Western blot analyses

To collect supernatant proteins, overnight cultures of one representative strain of CC15 (MIC 6935), CC8 (MIC 6947), CC45 (MIC 6981), and CC30 (MIC 6982) grown in 50 mL of TSB-glucose 0.25% (TSB-gluc) were pelleted by centrifugation at 4500 rpm for 30 min, at 4 °C and the supernatant was collected and centrifuged again. Culture supernatants were filtered and precipitated at 4 °C using 10% (v/v) trichloroacetic acid (Sigma-Aldrich, St Louis, MO, USA) for 1 h. The samples were centrifuged twice at 4000 rpm for 2 h at 4 °C and the supernatant was discarded. The pellets were resuspended in 800 μL ice-cold ethanol (96%) and then centrifuged at 14,000 rpm for 20 min at 4 °C. Resulting pellets were air dried at room temperature and proteins were solubilized with 100 μL of 8 M urea (Amresco, Dallas, TX, USA) for 30 min at room temperature. Protein concentration was quantified using a Bicinchoninic Acid Kit (BCA) (Sigma-Aldrich, St Louis, MO, USA).

CWA proteins from *S. aureus* clinical isolates were prepared as previously described [32]. In brief, overnight cultures of each of the above-selected strains grown in 5 mL of TSB-gluc were pelleted by centrifugation at 4500 rpm for 30 min, at 4 °C, washed with 1 mL of PBS and resuspended in 100 μL of isosmotic digestion buffer (phosphate--buffered saline (PBS) containing 26% [wt/vol] raffinose; Sigma-Aldrich, St Louis, MO, USA). CWA proteins were solubilized by adding 1.5 μL of a 1 mg/mL solution of lysostaphin (Sigma-Aldrich, St Louis, MO, USA) and incubation with shaking at 37 °C for 2 h. Samples were centrifuged at 8000×*g* for 30 min with slow deceleration and the supernatant was taken as the cell wall fraction. Protein concentration was quantified using a Bicinchoninic Acid Kit (BCA) (Sigma-Aldrich, St Louis, MO, USA).

For detection of cytoplasmic GFP, overnight cultures of *S. aureus* 132

containing pCN52:P_{xx}CC plasmids were diluted 1:100 and cultured in 25 ml TSB-gluc at 37 °C under static conditions for 5 h. Cells were pelleted by centrifugation at 4500 rpm for 30 min at 4 °C, washed with 1 mL of PBS, suspended in 400 μL PBS and lysed using a FastPrep-24™ 5G homogenizer (MP Biomedicals, LLC, Irvine, CA, USA). The total amount of protein was quantified using a Bradford protein assay kit (Bio-Rad, Hercules, CA, USA).

For Western blot analysis, equal amounts of protein per sample were loaded on a 12% Stain-Free FastCastTM Acrylamide Kit, 12% (Bio-Rad, Hercules, CA, USA) after adding a volume of Laemmli buffer and boiling for 5 min. After the electrophoresis, the samples were transferred to Amersham™ Protran™ Premium 0.45 μm nitrocellulose blotting membranes (Cytiva, Marlborough, MA, USA) by electroblotting. Membranes were blocked overnight in PBS containing 0.1% Tween 20 and 5% skimmed milk under shaking conditions and incubated with rabbit *anti-S. aureus* polyclonal antibody that reacts with soluble and structural antigens of the whole bacterium (Bio-Rad, Hercules, CA, USA) at 1 μg/mL in blocking solution for 1 h at room temperature. For GFP detection, the membranes were incubated with *anti*-GFP antibodies (Living Colors A.v. monoclonal antibody JL-8 (Clontech, Mountain View, CA, USA), diluted 1:2500 in blocking solution for 2 h at room temperature. Alkaline phosphatase-conjugated goat anti-rabbit immunoglobulin G (Thermo Scientific, Waltham, MA, USA) diluted 1:5000 in blocking solution was used as a secondary antibody and the subsequent chemiluminescence reaction was recorded with ECL Prime western blotting detection reagents (Cytiva, Marlborough, MA, USA) in the Chemidoc™ MP Imaging System (Bio-Rad, Hercules, CA, USA).

2.5. Generation of posttranscriptional fusions of adhesin-encoding genes IGRs with gfp

To generate posttranscriptional fusions of the regulatory regions (promoter and 5' UTR) of adhesins encoding genes and the *gfpmut2* gene [33], the region comprising two hundred nucleotides immediately upstream of each gene coding sequence was amplified from one representative strain of CC15 (MIC 6935), CC8 (MIC 6947), CC45 (MIC 6981), and CC30 (MIC 6982), using primers listed in Supplementary Table S3 for each adhesin-encoding gene. The PCR products were cloned into the pJET 1.2 vector and then sub-cloned into the pCN52 plasmid [33] digested with *Sal*I and KpnI, giving plasmids pCN52:P_{xx}CC that were transformed into the *S. aureus* 132 strain.

2.6. Construction of sortase mutants

To construct the sortase A (*srtA*) mutants, two DNA fragments were amplified with the primer pairs BG_STAP79/LM97 and LM98/BG_STAP86 (Supplementary Table S3) from the MW2 wild type strain. The two PCR fragments were fused through overlapping PCR using primers BG_STAP79 and BG_STAP86, cloned into the pJET 1.2 vector and then subcloned into the pMAD vector [34] digested with NcoI and BamHI, generating plasmid pMAD:*srt*A_{AD}. This plasmid was transformed into the MIC 6947, MIC 6981 (purified from *S. aureus* RN4220) [35], and MIC 6982 (purified from *E. coli* IM30B) wild-type strains by electroporation [36]. Homologous recombination experiments were performed as previously described [37]. Erythromycin-susceptible white colonies, which did not further contain the pMAD plasmid, were tested by PCR using the primers BG_STAP86 and BG_STAP87 and sanger sequencing was used to confirm the generated isogenic mutants.

2.7. Co-infection experiments

To evaluate *in vivo* colonization, we used a murine model of catheter-associated biofilm. Bacteria grown overnight in TSB were suspended in PBS to an OD_{600nm} of 0.2 (10^8 CFU/mL). A total of 24 five-week-old ICR female mice (Envigo, Indianapolis, IN, USA) were anesthetized with isoflurane, and two 15 mm intravenous catheters (24G; B. Braun Medical, Bethlehem, PA, USA) were implanted into the subcutaneous interscapular of each mouse, and co-infected by injection of 100 μL (a total of 10^7 CFU) of a bacterial mixture, containing the same proportion of each *S. aureus* strain (CC15 (MIC 6935), CC8 (MIC 6947), CC45 (MIC 6981), and CC30 (MIC 6982)). Five days after infection, animals were anesthetized by isoflurane inhalation and euthanatized by cervical dislocation. The catheters were removed aseptically and placed in Lysing Matrix E tubes (Thermo Scientific, Waltham, MA, USA) containing 1 mL of TES, and cells were lysed using a FastPrep-24™ 5G homogenizer (MP Biomedicals, LLC, Irvine, CA, USA) to isolate the DNA.

Extracted DNA was used for library preparation using Illumina Amplicon Library kit MS-102-3003 (Illumina, San Diego, CA, USA) followed by Illumina sequencing at Fisabio (Valencia, Spain) on a MiSeq System Illumina sequencer (San Diego, CA, USA) using a paired-end approach. The oligonucleotides LM63/LM64 and LM99/LM100 (Supplementary Table S3) were designed for P*sasJ,* and P*clfB* amplicon sequencing, respectively. DNA amplicon libraries were generated using a limited cycle PCR: initial denaturation at 95 °C for 3 min followed by 25 cycles of annealing (95 °C 30 s, 55 °C 30 s, 72 °C 30 s) and extension at 72 °C 5 min, using a KAPA HiFi HotStart ReadyMix (KK2602) (Sigma-Aldrich, St Louis, MO, USA). Then, Illumina sequencing adaptors and dual-index barcodes (Nextera XT index kit v2, FC-131-2001) were added to the amplicons. Libraries were normalized and pooled before sequencing. Quality assessment was performed by the use of the fastp program [38] applying the following parameters: min_length: 50; trim_qual_right: 30; trim_qual_type: mean; and trim_qual_window: 10. R1 and R2 from Illumina sequences were joined using the *FLASH* program applying default parameters [39]. Reports, graphs, and statistics were obtained using the ea-utils programs suite [40]. The MultiQC report was produced using the *MultiQC* program [41]. The Sequence Read Archives (SRAs) with detailed information of the samples were deposited in NCBI under the BioProject accession number PRJNA834761.

Sequence mapping was carried out with the software BWA v.0.7.17-r1188 and the variants within the reads were located with the software ivar v.1.3.1. For the feature counts, a bash script was written to count the number of reads that mapped to each specific sequence. The number of reads was used to determine the percentage of read abundance. Statistical analyses were performed with the GraphPad Prism v9.2.0 program. One-way ANOVA was used followed by Tukey's multiple comparisons. In all tests, p values of less than 0.05 were considered statistically significant: $^{*}p < 0.05$, $^{**}p < 0.01$, $^{***}p < 0.001$, and $^{****}p < 0.0001$.

2.8. Biofilm formation phenotypes on protein precoated surfaces

To determine differences in initial adhesion between strains, a biofilm formation assay on protein pre-coated polystyrene plates was performed. First, Fn, Fibrinogen (Fg) and von Willebrand factor (VWF) were dissolved in buffer sodium carbonate 40 mM at a concentration of 5 μg/mL. Then, 100 μL of the corresponding coating was added to wells of a 48-well Nunclon™ Delta surface microtiter plate (Thermo Scientific, Waltham, MA, USA). After overnight incubation at 4 °C under shaking, the plate was rinsed once with water and the biofilm formation assays were performed. Briefly, overnight cultures were adjusted to an OD_{546nm} of 0.13 (10^8 CFU/mL) in TSB-gluc and further diluted 1:1000. An inoculum consisting of 1 mL of each diluted suspension (10^5 CFU/mL) was added to the pre-coated wells. After 5 h of static incubation at 37 °C, wells were rinsed once with water, dried, and stained with 1 mL of crystal violet for 5 min (VWR, Radnor, PA, USA). To quantify stained cells, 1 mL of ethanol-acetone (80:20, vol/vol) was added to each well, 500 μL of the suspension were transferred to a new 48-well plate and the OD_{595nm} was recorded in a FLUOstar Omega (BMG LABTECH, Ortenberg, Germany) microplate reader. Six biological replicates with two technical replicates were used.

2.9. Ethics statement

All animal studies were reviewed and approved by the Comité de Ética para la Experimentación Animal (CEEA) of the Universidad de Navarra (approved protocol 032-17). The experiments were performed at the Centro de Investigación Médica Aplicada (ES312010000132) under the principles and guidelines described in the European Directive 2010/63/EU for the protection of animals used for experimental purposes.

3. Results

3.1. Identification of genetic variations in the regulatory regions of genes encoding surface adhesins

Surface adhesins play an important role in the initial attachment to plasma proteins that cover the surface of prosthetic devices after implantation [19,20,42]. We explored if the differences in the presence and/or expression levels of genes encoding surface adhesins in clinical isolates of *S. aureus* might modulate the initial attachment and capacity of *S. aureus* to colonize implanted prosthetic devices. To explore this hypothesis, we examined a collection of clinical strains isolated from PJI (n = 45) and wounds (n = 26) [28] (Supplementary Fig. S1) for the presence/absence of twenty-three genes encoding CWA proteins and non-covalently associated surface proteins of the SERAM family. The results revealed that the genes *fnbA, clfA, clfB, sdrC, spa, sasC, sasE* (*isdA*), *sasF, sasH* (*adsA*), *sasI* (*isdH*), *sasJ* (*isdB*), *eap, emp, vwb* and *efb* were present in all strains, whereas the genes *fnbB, cna, sdrD, sdrE, sasA* (*srAp*), *sasD, sasG* and *fmtB* (*sasB*) were absent in some of them (Table 1). For instance, isolates from lineages CC15 and CC5 and most of the isolates from CC8 (93%) contained *sasG*, whereas none of the isolates from CC30 and CC45 contained this gene. On the contrary, the *cna* gene was present in all the isolates from CC45 and CC30 and was absent in CC15, CC5 and most of the CC8 (86%) isolates (Table 1). With respect to genes whose presence varied within the same lineage, no correlation was observed between their presence/absence and the source of infection (PJI or wounds).

We next explored the possibility that genetic variations between isolates might be located in the regulatory regions (romoter and 5' UTR) controlling the expression of adhesin proteins. Thus, we compared a sequence of 200 nt upstream the first codon of each of the 15 genes encoding surface adhesins present in all the strains with the corresponding sequence in the reference genome of *S. aureus* MW2 strain (CC1). The conservation rate of the sequence in the regulatory regions was highly variable depending on the gene (Fig. 1 and Supplementary Fig. S2). The sequence of the regulatory region of *sasE* and *fnbA* genes was highly conserved with variation rates below 5%. In contrast, the sequence of the regulatory region of *sdrC* showed a variation rate of 28% (Supplementary Table S4). Notably, the SNPs were highly conserved between isolates of the same sequence type, regardless of whether the strain was isolated from PJI or wounds. Taken together, these results indicated that SNPs variations in the regulatory region of surface adhesin genes are characteristic of each *S. aureus* ST lineage.

3.2. Contribution of SNPs to surface adhesins expression

We next wondered whether the SNPs present in IGRs may have an impact on surface adhesins expression levels. For that, we first used a commercial polyclonal antibody (Bio-Rad, Hercules, CA, USA) raised against soluble and structural antigens of the whole bacterium to compare the overall expression levels of CWA and secreted proteins between selected strains from different CC: CC15 (MIC 6935), CC8 (MIC 6947), CC45 (MIC 6981), and CC30 (MIC 6982). To identify the CWA proteins, we constructed sortase A (*srtA*) mutants for each strain. Our reasoning was that those bands that disappear in the absence of the SrtA activity would correspond to CWA proteins; regarding secreted proteins,

Table 1
Prevalence of genes encoding surface adhesins in PJI and wounds isolates.[a].

	CC (*n*)	ST (*n*)	Prevalence (%)							
			fnbB	***cna***	***sdrD***	***sdrE***	***sasA***	***sasD***	***sasG***	***fmtB***
PJI	**CC45 (12)**	ST45 (12)	75	100	83	83	100	100	0	100
	CC30 (8)	ST30 (8)	88	100	100	88	100	100	0	100
	CC8 (6)	ST8 (1)	100	0	100	100	100	100	100	100
		ST630 (4)	75	0	100	75	0	100	100	100
		ST789 (1)	100	0	100	100	100	100	100	100
	CC15 (6)	ST15 (5)	100	0	100	100	100	100	100	100
		ST3457 (1)	100	0	100	100	100	100	100	100
	CC5 (3)	ST5 (3)	100	0	100	100	100	100	100	100
	CC22 (1)	ST22 (1)	0	100	100	0	0	0	100	100
	CC1 (1)	ST1 (1)	100	0	100	100	100	100	0	100
		ST50 (2)	100	100	100	100	100	100	0	100
		ST20 (2)	50	0	50	100	100	100	100	100
		ST25 (1)	100	100	100	100	100	100	0	100
		ST80 (1)	100	0	100	0	100	100	0	100
		ST50 (1)	100	0	0	100	100	100	100	100
		ST182 (1)	100	100	0	0	100	0	100	0
Wounds	**CC8 (8)**	ST8 (2)	100	0	100	100	100	100	50	100
		ST254 (1)	100	0	100	0	100	100	100	100
		ST247 (3)	33	0	100	33	100	100	100	100
		ST239 (2)	100	100	100	50	100	100	100	100
	CC30 (3)	ST30 (3)	33	100	100	100	100	100	0	100
	CC5 (3)	CC5/ST5 (1)	100	0	100	100	100	100	100	100
		CC5/ST225 (1)	100	0	100	100	100	100	100	100
		CC5/ST1649 (1)	100	0	100	100	100	100	100	100
	CC45 (1)	ST45 (1)	0	100	100	100	100	100	0	100
	CC15 (1)	ST15 (1)	100	0	100	100	100	100	100	100
		ST25 (3)	100	0	100	100	100	100	0	100
		ST80 (3)	33	0	100	100	100	100	100	100
		ST182 (2)	100	100	0	0	100	0	100	0
		ST121 (1)	100	100	100	100	100	0	0	100
		ST1693 (1)	0	100	100	100	100	0	0	100

[a] The *fnbA, clfA, clfB, sdrC, spa, sasC, sasE, sasF, sasH, sasI, sasJ, eap, emp, vwb* and *efb* genes are not included because they are present in all strains.

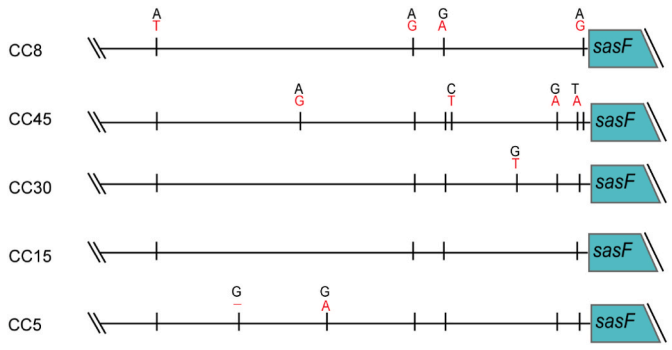

Fig. 1. Analysis of genetic variations in the regulatory region controlling the expression of surface adhesins. The region controlling *sasF* expression is shown as an example. PJI and wound isolates were grouped into twelve different clusters according to the SNPs present in the region comprising 200 nt upstream of the *sasF* gene compared to the sequence of the reference strain MW2. The most representative sequence variant for the most prevalent clonal complexes is shown. The black lines show the SNPs or indels found. All sequence variations found in CC8 are depicted (nucleotide changes from a black to a red nucleotide in the upper strand). In the rest of CCs, only sequence variations that are different from the ones found above are detailed. Eleven SNPs were identified among the representative sequence variants; none of the strains contained the same sequence as the MW2 reference strain.

no differences between wild-type and isogenic *srtA* mutants should be observed, therefore secreted proteins profiles are shown as a control. We generated *srtA* mutants for CC18, CC45 and CC30 strains. However, we were unable to genetically manipulate and generate the *srtA* mutant in the CC15 strain. Western Blot analysis revealed differences in the levels of CWA proteins between isolates of different CCs (Supplementary Fig. S3).

To specifically investigate the contribution of the SNPs in IGRs to the expression of surface adhesins without the interference of particular regulators that control the expression of surface adhesins in each strain, the region encompassing 200 nt upstream of the first codon of each adhesin-encoding gene present in the representative PJI isolates of CC15, CC8, CC45 and CC30 was fused with the *gfp* gene in the pCN52 plasmid. Then, the resulting plasmids were inserted in the *S. aureus* 132 strain, which is able to produce a proteinaceous-biofilm matrix when grown in TSB-glucose medium [43]. The effect of the genetic variations in IGRs on GFP expression levels was analyzed by Western blot. The results revealed large differences in the expression level of each surface adhesin. Of note, in general, expression from the regulatory region of *spa, clfA, clfB*, *vwb* and *efb* genes was high when compared to other regions such as the ones controlling expression of *sdrC*, *sasC*, *sasE*, *sasI*, *sasJ*, *eap* and *emp* (Fig. 2).

Next, we compared the expression of *gfp* under the regulatory region of each surface adhesin-encoding gene amongst the four different CCs. The results showed variability in the expression pattern of *spa, sdrC, sasC, sasF, sasH, sasI, sasJ, emp, eap, vwb* and *efb* genes, indicating that the SNPs present in the regulatory regions of the genes encoding for surface adhesins affect their expression levels (Fig. 3). The level of expression of *fnbA, clfA, clfB* and *sasE* genes remained unchanged among the isolates of different CCs, indicating that the SNPs present in the regulatory region of these genes were not involved in transcriptional and/or post-transcriptional regulation of such genes expression. Collectively, these results provided robust evidence that surface adhesin expression levels vary among *S. aureus* ST lineages due to sequence variations in IGRs of the corresponding genes.

3.3. Comparison of the in vivo colonization capacity of S. aureus isolates of different CCs

Taking into account the above results demonstrating that the strength of the promoters encoding for surface adhesins varies between *S. aureus* isolates of different CCs, we hypothesized that differences in the capacity to colonize implanted prostheses might occur. To investigate this possibility, we carried out an *in vivo* catheter colonization assay with a mixture containing four strains representative of the four CCs that most frequently caused prosthesis infections in our PJI collection. An intrinsic difficulty in co-infection experiments is that a selective analytical method is required in order to distinguish and quantify each strain in the mixture. To address this methodological challenge, we amplified a 200 nt region upstream of the *sasJ* and *clfB* genes that contain the specific SNPs of each CC (Fig. 4A) [44]. To validate the selected DNA signatures, we prepared *in vitro* mock mixtures containing different proportions of the four isolates, total DNA was purified, PCR

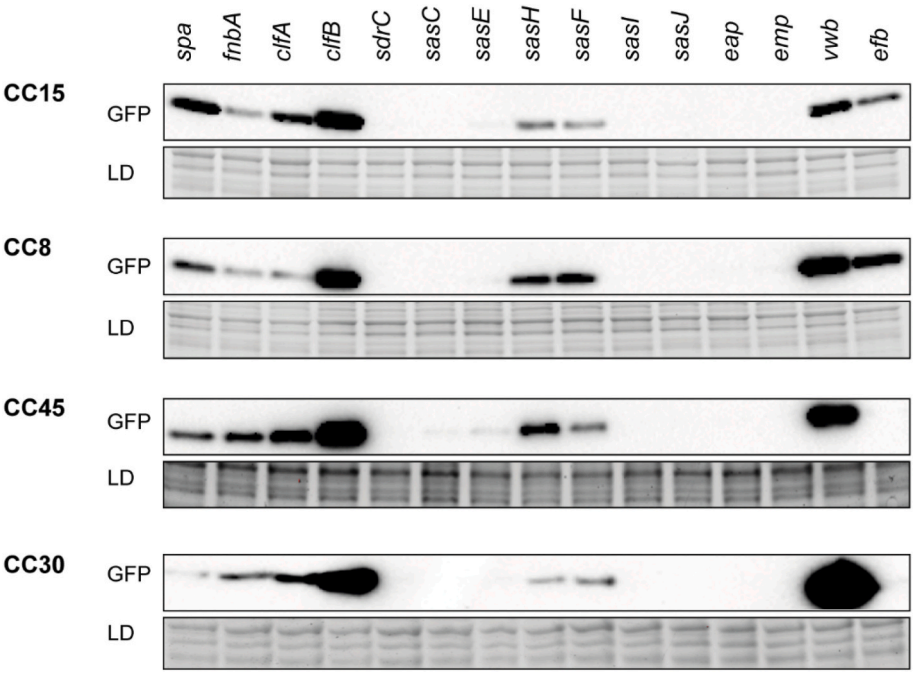

Fig. 2. Comparison of surface adhesins expression levels within the same strain. Western blots show GFP protein levels in *S. aureus* 132 strain transformed with plasmids containing reporter fusions of 200 nt upstream the initial codon of 15 surface adhesin-encoding genes, amplified from the same isolate, with the *gfp* gene. One representative *S. aureus* PJI isolate of each of the four most abundant clonal complexes CC15, CC8, CC45 and CC30 was used for amplification of regulatory sequences. Bacteria were grown until the exponential phase and proteins were transferred to nitrocellulose membranes, incubated with *anti*-GFP monoclonal antibodies and developed using peroxidase-conjugated goat anti-mouse antibodies and a bioluminescence kit. Stain-free gels are shown as loading controls (LD).

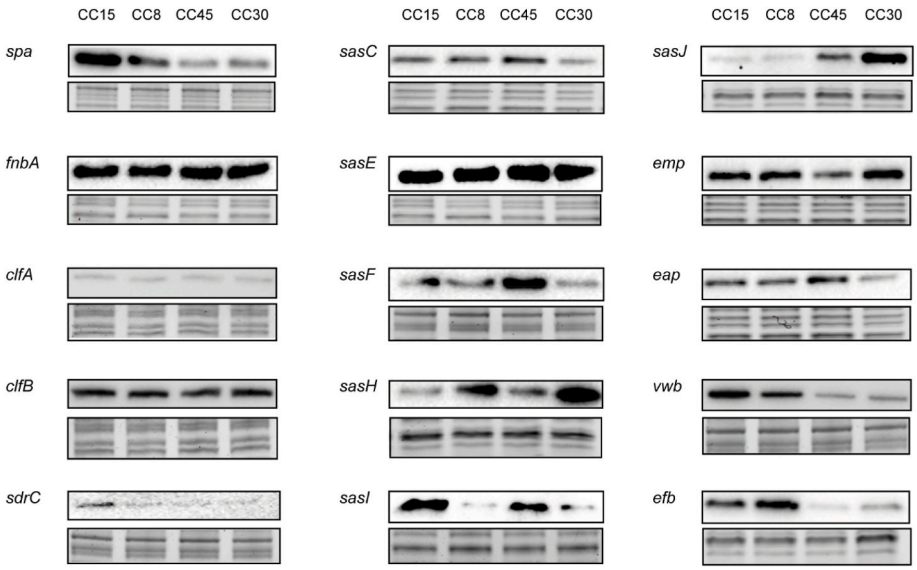

Fig. 3. Comparison of surface adhesins expression levels in strains from different CCs. Western blots show GFP protein levels in *S. aureus* 132 strain transformed with plasmids containing reporter fusions of 200 nt upstream the initial codon of each surface adhesin-encoding genes, amplified from representative *S. aureus* PJI isolates of the four most abundant CCs, with the *gfp* gene. Bacteria were grown until the exponential phase and proteins were transferred to nitrocellulose membranes, incubated with *anti*-GFP monoclonal antibodies and developed using peroxidase-conjugated goat anti-mouse antibodies and a bioluminescence kit. Membrane exposure was adjusted in each case to allow band visualization in all cases. Stain-free gels are shown as loading controls.

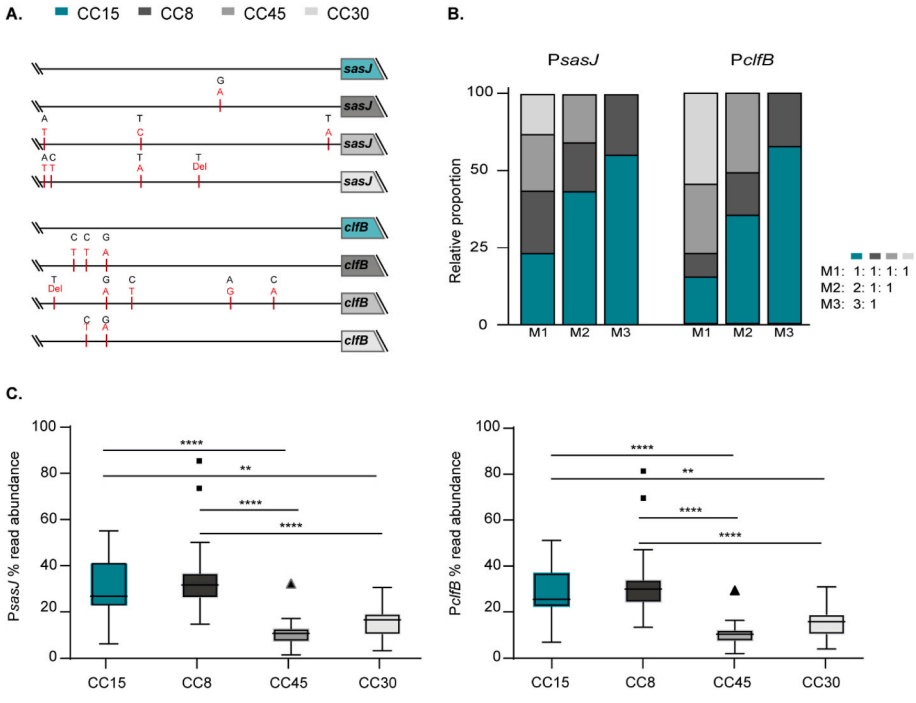

Fig. 4. DNA signatures for quantifying isolates from different clonal lineages during co-infection experiments of catheters in a mouse model. (**A**) Natural sequence variants of the regulatory regions of *sasJ* and *clfB* genes from representative strains ascribed to CC15, CC8, CC45, and CC30. The red lines show the SNPs or indels found compared with the CC15 sequence (nucleotide changes from a black to a red nucleotide in the upper strand). (**B**) Relative proportion of each isolate based on the number of reads corresponding to sequence variants. The results represent the mean of three independent *in vitro* experiments ($n = 3$). M1: Mixture one (equal proportion of each of the four strains); M2: Mixture two (double proportion of CC15 strain than CC8 and CC45); M3: Mixture three (triple proportion of CC15 strain than CC8). (**C**) Differences in colonization capacity of *S. aureus* isolates from different clonal complexes in a murine model of catheter colonization. Percentage of reading abundance after 5 days of infection according to the number of reads of sequence variants of *sasJ* and *clfB* regulatory regions. Catheters were coinfected with equal amounts (10^7 CFU) of representative *S. aureus* PJI isolates ascribed to the most prevalent clonal complexes. CC15: MIC 6935; CC8: MIC 6947; CC45: MIC 6981; CC30: MIC 6982. The boxes indicate the range between the first and third quartiles (25th and 75th percentiles). The horizontal line inside the box is the median. The size of the box represents the interquartile range (IQR). The whiskers indicate the spread of data outside the box at up to 1.5 times the IQR from the edge of box (1.5 times the size of the box below the 25th percentile or above the 75th percentile). Data further than 1.5 times the IQR from the box are designated outliers and plotted individually. Statistically significant differences were determined using one-way ANOVA, followed by Tukey's multiple comparison (**, $p < 0.01$), (***, $p < 0.001$) (****, $p < 0.0001$).

amplified and sequenced. The reads were processed and mapped to *sasJ* and *clfB* regions. The total number of reads that passed a quality filter was higher than 99% for both P*sasJ* and P*clfB*, respectively. The results confirmed that the number of mapped reads obtained corresponding to each DNA signature was proportional to the amount of each bacterium in the original mixture (Fig. 4B). We next used this strategy to determine the proportion of each isolate on the surface of catheters implanted in the subscapular space of mice. A mixture of equal numbers (10^7 CFU) of the four representative strains was used to colonize the implanted catheters (Supplementary Fig. S4) and after five days, catheters were recovered, DNA was purified, and the amount of each bacterium was quantified based on the abundance of reads for each DNA signature. The results revealed that read abundance corresponding to strains from CC15 and CC8 was significantly higher than the reads corresponding to strains from CC45 and CC30 (Fig. 4C). No significant differences were found between the number of reads corresponding to CC15 and CC8 strains and CC30 and CC45 strains. Together, these results evidenced that *S. aureus* isolates show CC dependent variation of the capacity to

colonize an implanted catheter.

If differences in the ability of the strains from the different clonal groups to adhere to implanted catheters were due to differences in their adhesion to plasma proteins coating the catheter surface, similar variances in their capacity to adhere to abiotic surfaces covered with plasma proteins *in vitro* could be expected. To explore this hypothesis, we performed primary attachment assays on polystyrene pre-coated with Fn, Fg and VWF (Fig. 5). The results revealed that the representative strains from CC15 and CC8 showed a significantly higher capacity than isolates from CC30 and CC45 to adhere to polystyrene surfaces coated with Fn and Fg, whereas in the case of surfaces coated with VWF, all isolates showed a similar primary adhesion capacity. Interestingly, isolates from CC15 and CC8 lineages also showed a higher capacity to adhere to uncoated polystyrene surfaces than isolates from CC30 and CC45. Notably, adhesion of CC15 and CC8 isolates to the uncoated surface was lower than to Fn and Fg coated surfaces. Together, these results demonstrated that the strains winning the race for colonization of the surface of the implant *in vivo* also displayed a higher capacity to colonize abiotic surfaces coated with plasma proteins *in vitro*.

4. Discussion

PJI is the most severe complication following arthroplasty [45]. *S. aureus* is known as the main bacterium causing PJI due to its ability to adhere to and establish biofilms on abiotic surfaces [13,46]. Epidemiologic studies have shown that several *S. aureus* lineages can cause PJI [47,48]. However, the fact that strains from different clonal complexes are isolated from PJI does not necessarily mean that isolates from different CCs have the same ability to adhere irreversibly to the implant surface and cause an infection.

A simple mechanism to generate variability in the capacity to colonize implants between different isolates may be due to variations in the presence/absence of adhesin-encoding genes [49,50]. For instance, SasG, a protein important in promoting biofilm formation during the accumulation phase, is present in strains of CC15 and CC8 whereas it is absent in strains from CC30 and CC45 [51,52]. On the contrary, the presence of the collagen-binding protein (Cna) has been mainly associated with strains from CC30 and CC45 [53]. The analysis of the genome sequences of our collection of PJI isolates confirmed the presence of *fnbA, clfA, clfB, sdrC, spa, sasC, sasE, sasF, sasH, sasI, sasJ, eap, emp, vwb* and *efb* in all the isolates. In agreement with previous studies, the *sasG* gene was found in all PJI strains from CC8 and CC15 and was not detected in any CC30 and CC45 isolate, whereas *cna* was present in all strains from CC30 and CC45 and absent in all CC15 and CC8 PJI isolates. Our results revealed that the selected strains from CC8 and CC15 showed a higher capacity to colonize catheters *in vivo* and a higher ability to form a biofilm on protein precoated surfaces than isolates from CC30 and CC45, and therefore we cannot exclude that the presence of SasG might contribute to an increased *S. aureus* propensity to colonize and accumulate on the surface of implanted prostheses. Following the same reasoning, our findings suggest that the presence of Cna may not be as important when competing to colonize a surface.

A second source of variability in the ability of *S. aureus* to colonize implants can be generated by changes in the sequence of adhesin proteins. It is well known that the exposure of the bacteria to the pressure of the host immune system contributes to the accumulation of polymorphisms within surface proteins. Studies on *S. aureus* have revealed that clinical isolates accumulate SNPs in their surface proteins as the infection progresses [48,54]. Ma et al. showed that increasing genotypic variation in adhesin-encoding genes between the first and later isolates from PJI outcomes with changes in the ability to bind to plasma proteins. These changes might confer advantages to successfully colonizing surfaces and/or evading the immune system. Similarly, several studies have evidenced that polymorphisms in FnBPA-binding repeats in isolates causing infection of cardiovascular devices are associated with an enhanced capacity to adhere to Fn [23,55,56].

A third level of variability can be generated through mutations at the IGRs of certain genes that cause changes in the expression levels of compounds important for implant colonization. Most studies dedicated to investigating how bacteria adapt to the host environment have focused on changes that occur within coding regions, whereas the role of intergenic mutations has remained mostly disregarded. Importantly, several evolution studies have shown that mutations in the regulatory elements upstream of transcriptional start sites cause changes in the transcription levels of genes important for evolution of pathogenic phenotypes, including essential genes that are less permissive to accumulate mutations in the coding sequence [57–59]. In the case of *S. aureus*, SNPs accumulation in the IGRs of adhesin-encoding genes present in strains isolated from later points of infection has been described [48]. On the contrary, regarding the production of the main exopolysaccharide of the *S. aureus* biofilm matrix, SNPs in the highly conserved IGRs of the *icaADBCR* operon were not associated with changes in *icaADBC* expression, PIA/PNAG production and adaptation to PJI [29].

A fourth level of variability can be generated by changes in the expression levels of global transcriptional regulators controlling the expression of surface adhesins. Several regulatory elements, such as *agrAC, saeRS, arlRS, mgrA*, and *sarA* are known to directly or indirectly regulate the expression of staphylococcal adhesins in response to different environmental conditions [26]. For instance, the *agr* system represses adhesins expression and its activity is inhibited by proteins found in human serum and blood [60]. Thus, the *agr*-dependent expression of adhesins is inhibited in plasma or human serum. Similarly, SaeRS, Agr, and SarA, upregulate the expression of some SERAMs such as *eap* and *emp* under low-iron conditions [26,61]. SarA also responds to O_2 or CO_2 levels and can induce (*fnbA and fnbB*) or repress (*spa*) the expression of some adhesins either in an *agr*-dependent or independent way [62]. Moreover, the repression of the protease activity by SarA can affect the accumulation of some staphylococcal proteins [63].

In the present study, the comparison of the IGRs upstream 15 adhesin-encoding genes of the 71 isolates under study revealed strong differences in conservation rates. In particular, the IGR upstream the

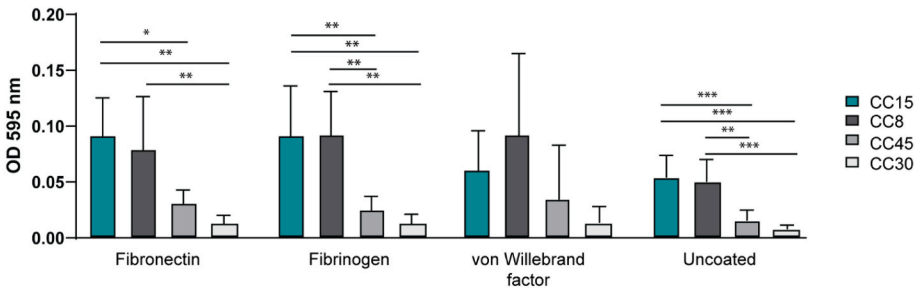

Fig. 5. Biofilm biomass formed by representative *S. aureus* PJI isolates from CC15, CC8, CC45 and CC30 on protein coated surfaces. The wells of polystyrene plates were pre-coated with 5 μg/mL of fibronectin, fibrinogen, and the von Willebrand factor and kept overnight at 4 °C. Static biofilms were grown in TSB-gluc on the pre-coated 48-well plates for 5 h. Biofilm formation was quantified by crystal violet staining, followed by 80:20 ethanol: acetone elution and OD_{595nm} measurement. The data represent the mean of six biological replicates ($n = 6$) with two technical replicates; error bars represent ± SD. Statistically significant differences were determined using one-way ANOVA, followed by Tukey's multiple comparisons (*, $p < 0.05$), (**, $p < 0.01$)), (***, $p < 0.001$).

fnbA gene was highly conserved, only comprising seven SNPs, whereas the IGR upstream *sdrC* accumulated 56 SNPs that resulted in a 28% variation rate. The high degree of conservation in the IGR upstream *fnbA* was somehow unexpected because the FnBPA amino acid sequence varies considerably between *S. aureus* lineages [64] and polymorphisms associated with binding mechanisms have been described in isolates from cardiovascular devices infections [55]. A significant difficulty for inferring the functional value of SNPs in IGRs compared to those in coding regions is that the synonymous/non-synonymous distinction does not apply for IGRs. Thus, experimental evaluation of the impact of each set of mutations becomes necessary in order to reach a conclusion on its function and relevance. Here, the potential functional relevance of the SNPs in the IGRs of the 15 adhesins encoding genes to their expression was determined using posttranscriptional fusions with the *gfp* reporter gene. The results showed that each CC shows a characteristic profile of adhesins expression. The Spa, vWbp and Efb reporters showed a higher level of expression in CC15 and CC8 isolates compared to CC30 and CC45 strains. Protein A (Spa) has been shown to promote catheter-associated infection [65], and the secreted VWF-binding protein (vWbp) promotes ClfA-mediated adhesion to VWF [66]. The Efb is a very large secreted protein that binds host Fg and complement C3 and plays an important role in evasion of the immune system [67]. On the other hand, the presence of SNPs in the IGRs upstream of genes encoding for FnBPA, ClfA, and ClfB did not affect expression levels, suggesting that the SNPs were silent, at least in the conditions tested.

Based on the notion that *S. aureus* colonization capacity of prosthetic implants is very likely due to the expression profile of the whole family of surface adhesins, we explored if *S. aureus* isolates from different CCs, with a particular profile in the presence and SNPs of adhesins genes, might show an advantage in colonizing an implant, using a catheter infection model in mice. At the same time, aiming to apply the reduction principle for ethical use of animals in scientific research [68], we coinfected each catheter with a mixture containing equal numbers of representative strains of four CCs. Because the four isolates were genetically very closely related, it was necessary to design oligonucleotides that amplify DNA regions containing enough number of SNPs to unambiguously distinguish and quantify the amount of bacteria corresponding to each isolate on the surface of the catheter after the infection process. Once we selected the regions comprising IGRs of *sasJ* and *clfB* genes, we applied the well-established methodology used to sequence and characterize microbiomes using 16S amplification products. Interestingly, isolates from CC15 and CC8 showed a higher capacity to colonize the catheters surface than isolates from CC30 and CC45. These results corresponded to the ability of each isolate to adhere to abiotic surfaces coated with individual plasma proteins, strongly suggesting that differences in the capacity to colonize implanted devices might result from the sum of adhesion properties of each individual adhesin.

We anticipate that this experimental approach for quantifying and detecting closely related bacterial isolates will be very helpful to identify competitive advantages for certain clinical bacterial isolates in specific stages of the infectious process or in polymicrobial biofilm research.

CRediT authorship contribution statement

Liliana Morales-Laverde: Investigation, Visualization, Methodology, Validation, Writing – original draft. **Margarita Trobos:** Methodology, Writing – review & editing, Resources, Funding acquisition. **Maite Echeverz:** Investigation. **Cristina Solano:** Writing – review & editing, Supervision. **Iñigo Lasa:** Conceptualization, Writing – review & editing, Supervision, Project administration, Funding acquisition.

Declaration of competing interest

The authors declare that they have no known competing financial interests or personal relationships that could have appeared to influence the work reported in this paper.

Data availability

Data will be made available on request.

Acknowledgments

The authors would like to thank Prof. Ola Rolfson (Department of Orthopaedics, Institute of Clinical Sciences, University of Gothenburg, Sweden) and Assoc. Prof. Bodil Jönsson (Department of Infectious Diseases, Institute for Biomedicine, University of Gothenburg, Sweden) for the collection of the strains from periprosthetic joint infections. We thank Prof. Edward Moore (Culture Collection at the University of Gothenburg, CCGU, Sweden) for kindly providing the *S. aureus* strains from wounds. This work was financially supported by the Spanish Ministry of Science and Innovation grant PID2020-113494RB-I00 to I.L. (Agencia Española de Investigación/Fondo Europeo de Desarrollo Regional, European Union), the European Union's Horizon 2020 research and innovation program under the Marie Skłodowska-Curie grant agreement No 754412 [MoRE2020 - Region Väs-tra Götaland], and the IngaBritt and Arne Lundberg Foundation (LU2021-0048). L.M.L was supported by the European Union's H2020 research and innovation programme under Marie Sklodowska-Curie grant agreement No 801586 (IberusTalent).

Appendix A. Supplementary data

Supplementary data to this article can be found online at https://doi.org/10.1016/j.bioflm.2022.100093.

References

[1] Schürch AC, Arredondo-Alonso S, Willems RJL, Goering RV. Whole genome sequencing options for bacterial strain typing and epidemiologic analysis based on single nucleotide polymorphism versus gene-by-gene–based approaches. Clin Microbiol Infect 2018;24:350–4. https://doi.org/10.1016/j.cmi.2017.12.016.
[2] Raskin DM, Seshadri R, Pukatzki SU, Mekalanos JJ. Bacterial genomics and pathogen evolution. Cell 2006;124:703–14. https://doi.org/10.1016/j.cell.2006.02.002.
[3] Sheppard SK, Guttman DS, Fitzgerald JR. Population genomics of bacterial host adaptation. Nat Rev Genet 2018;19:549–65. https://doi.org/10.1038/s41576-018-0032-z.
[4] Toft C, Andersson SGE. Evolutionary microbial genomics: insights into bacterial host adaptation. Nat Rev Genet 2010;11:465–75. https://doi.org/10.1038/nrg2798.
[5] Du X, Larsen J, Li M, Walter A, Slavetinsky C, Both A, et al. Staphylococcus epidermidis clones express *Staphylococcus aureus*-type wall teichoic acid to shift from a commensal to pathogen lifestyle. Nat Microbiol 2021;6:757–68. https://doi.org/10.1038/s41564-021-00913-z.
[6] Viana D, Comos M, McAdam PR, Ward MJ, Selva L, Guinane CM, et al. A single natural nucleotide mutation alters bacterial pathogen host tropism. Nat Genet 2015;47:361–6. https://doi.org/10.1038/ng.3219.
[7] Sheppard SK, Didelot X, Meric G, Torralbo A, Jolley KA, Kelly DJ, et al. Genome-wide association study identifies vitamin B5 biosynthesis as a host specificity factor in *Campylobacter*. Proc Natl Acad Sci USA 2013;110:11923–7. https://doi.org/10.1073/pnas.1305559110.
[8] Pascoe B, Méric G, Murray S, Yahara K, Mageiros L, Bowen R, et al. Enhanced biofilm formation and multi-host transmission evolve from divergent genetic backgrounds in *Campylobacter jejuni*. Environ Microbiol. 2015;17:4779–89. https://doi.org/10.1111/1462-2920.13051.
[9] Arciola CR, Campoccia D, Montanaro L. Implant infections: adhesion, biofilm formation and immune evasion. Nat Rev Microbiol 2018;16:397–409. https://doi.org/10.1038/s41579-018-0019-y.
[10] Raafat D, Otto M, Reppschläger K, Iqbal J, Holtfreter S. Fighting *Staphylococcus aureus* biofilms with monoclonal antibodies. Trends Microbiol 2019;27:303–22. https://doi.org/10.1016/j.tim.2018.12.009.
[11] Speziale P, Pietrocola G, Foster TJ, Geoghegan JA. Protein-based biofilm matrices in *Staphylococci*. Front Cell Infect Microbiol 2014;4:171. https://doi.org/10.3389/fcimb.2014.00171.
[12] Foster TJ. Surface proteins of *Staphylococcus epidermidis*. Front Microbiol 2020;11:1829. https://doi.org/10.3389/fmicb.2020.01829.
[13] Otto M. Staphylococcal biofilms. Microbiol Spectr 2018;6. https://doi.org/10.1128/microbiolspec.gpp3-0023-2018.
[14] Schilcher K, Horswill AR. Staphylococcal biofilm development: structure, regulation, and treatment strategies. Microbiol Mol Biol Rev 2020;84. https://doi.org/10.1128/mmbr.00026-19.

[15] Montanaro L, Speziale P, Campoccia D, Ravaioli S, Cangini I, Pietrocola G, et al. Scenery of *Staphylococcus* implant infections in orthopedics. Future Microbiol 2011;6:1329–49. https://doi.org/10.2217/fmb.11.117.

[16] Puhto T, Puhto A-P, Vielma M, Syrjälä H. Infection triples the cost of a primary joint arthroplasty. Infect Dis Newsl 2019;51:348–55. https://doi.org/10.1080/23744235.2019.1572219.

[17] Heilmann C. Adhesion mechanisms of staphylococci, vol. 715. Dordrecht: Springer Netherlands; 2011. p. 105–23. https://doi.org/10.1007/978-94-007-0940-9_7.

[18] Geoghegan JA, Foster TJ. *Staphylococcus aureus*, microbiology, pathology, immunology, therapy and prophylaxis. Curr Top Microbiol 2015:95–120. https://doi.org/10.1007/82_2015_5002.

[19] Clarke SR, Foster SJ. Surface adhesins of *Staphylococcus aureus*. Adv Microb Physiol 2006;51:187–224. https://doi.org/10.1016/s0065-2911(06)51004-5.

[20] Foster TJ. The MSCRAMM family of cell-wall-anchored surface proteins of gram-positive cocci. Trends Microbiol 2019;27:927–41. https://doi.org/10.1016/j.tim.2019.06.007.

[21] Chavakis T, Wiechmann K, Preissner KT, Herrmann M. *Staphylococcus aureus* interactions with the endothelium: the role of bacterial "secretable expanded repertoire adhesive molecules" (SERAM) in disturbing host defense systems. Thromb Haemostasis 2005;94:278–85. https://doi.org/10.1160/th05-05-0306.

[22] Foster TJ, Geoghegan JA, Ganesh VK, Höök M. Adhesion, invasion and evasion: the many functions of the surface proteins of *Staphylococcus aureus*. Nat Rev Microbiol 2014;12:49–62. https://doi.org/10.1038/nrmicro3161.

[23] Casillas-Ituarte NN, Lower BH, Lamlertthon S, Fowler VG, Lower SK. Dissociation rate constants of human fibronectin binding to fibronectin-binding proteins on living *Staphylococcus aureus* isolated from clinical patients. J Biol Chem 2012;287:6693–701. https://doi.org/10.1074/jbc.m111.285692.

[24] Speziale P, Pietrocola G. The multivalent role of fibronectin-binding proteins A and B (FnBPA and FnBPB) of *Staphylococcus aureus* in host infections. Front Microbiol 2020;11:2054. https://doi.org/10.3389/fmicb.2020.02054.

[25] Roche F, Massey R, Peacock S, Day N, Visai L, Speziale P, et al. Characterization of novel LPXTG-containing proteins of *Staphylococcus aureus* identified from genome sequences. Microbiology 2003;149:643–54. https://doi.org/10.1099/mic.0.25996-0.

[26] Paharik AE, Horswill AR. The staphylococcal biofilm: adhesins, regulation, and host response. Microbiol Spectr 2016;4. https://doi.org/10.1128/microbiolspec.vmbf-0022-2015.

[27] Malchau KS, Tillander J, Zaborowska M, Hoffman M, Lasa I, Thomsen P, et al. Biofilm properties in relation to treatment outcome in patients with first-time periprosthetic hip or knee joint infection. J Orthop Transl 2021;30:31–40. https://doi.org/10.1016/j.jot.2021.05.008.

[28] Trobos M, Firdaus R, Malchau KS, Tillander J, Arnellos D, Rolfson O, et al. Genomics of *Staphylococcus aureus* and *Staphylococcus epidermidis* from periprosthetic joint infections and correlation to clinical outcome. Microbiol Spectr 2022. https://doi.org/10.1128/spectrum.02181-21. e02181-21.

[29] Morales-Laverde L, Echeverz M, Trobos M, Solano C, Lasa I. Experimental Polymorphism survey in intergenic regions of the *icaADBCR* Locus in *Staphylococcus aureus* isolates from periprosthetic joint infections. Microorganisms 2022;10:600. https://doi.org/10.3390/microorganisms10030600.

[30] Turner AB, Gerner E, Firdaus R, Echeverz M, Werthén M, Thomsen P, et al. Role of sodium salicylate in *Staphylococcus aureus* quorum sensing, virulence, biofilm formation and antimicrobial susceptibility. Front Microbiol 2022;13:931839. https://doi.org/10.3389/fmicb.2022.931839.

[31] Schenk S, Laddaga R. Improved method for electroporation of *Staphylococcus aureus*. FEMS Microbiol Lett 1992;73:133–8. https://doi.org/10.1016/0378-1097(92)90596-g.

[32] Arrizubieta MJ, Toledo-Arana A, Amorena B, Penadés JR, Lasa I. Calcium inhibits bap-dependent multicellular behavior in *Staphylococcus aureus*. J Bacteriol 2004;186:7490–8. https://doi.org/10.1128/jb.186.22.7490-7498.2004.

[33] Charpentier E, Anton AI, Barry P, Alfonso B, Fang Y, Novick RP. Novel cassette-based shuttle vector system for gram-positive bacteria. Appl Environ Microbiol 2004;70:6076–85. https://doi.org/10.1128/aem.70.10.6076-6085.2004.

[34] Arnaud M, Chastanet A, Débarbouillé M. New vector for efficient allelic replacement in naturally nontransformable, low-GC-content, gram-positive bacteria. Appl Environ Microbiol 2004;70:6887–91. https://doi.org/10.1128/aem.70.11.6887-6891.2004.

[35] Kreiswirth B, Lofdahl S, Betley M, O'Reilly M, Schlievert P, Bergdoll M, et al. The toxic shock syndrome exotoxin structural gene is not detectably transmitted by a prophage. Nature 1983;305:709–12. https://doi.org/10.1038/305709a0.

[36] Monk IR, Tree JJ, Howden BP, Stinear TP, Foster TJ. Complete bypass of restriction systems for major *Staphylococcus aureus* lineages. mBio 2015;6:e00308–15. https://doi.org/10.1128/mbio.00308-15.

[37] Valle J, Toledo-Arana A, Berasain C, Ghigo J, Amorena B, Penadés JR, et al. SarA and not σB is essential for biofilm development by *Staphylococcus aureus*. Mol Microbiol 2003;48:1075–87. https://doi.org/10.1046/j.1365-2958.2003.03493.x.

[38] Chen S, Zhou Y, Chen Y, Gu J. fastp: an ultra-fast all-in-one FASTQ preprocessor. Bioinformatics 2018;34:i884–90. https://doi.org/10.1093/bioinformatics/bty560.

[39] Magoč T, Salzberg SL. FLASH: fast length adjustment of short reads to improve genome assemblies. Bioinformatics 2011;27:2957–63. https://doi.org/10.1093/bioinformatics/btr507.

[40] Aronesty E. Comparison of sequencing utility programs. Open Bioinf J 2013;7:1–8. https://doi.org/10.2174/1875036201307010001.

[41] Ewels P, Magnusson M, Lundin S, Käller M. MultiQC: summarize analysis results for multiple tools and samples in a single report. Bioinformatics 2016;32:3047–8. https://doi.org/10.1093/bioinformatics/btw354.

[42] Anderson JM, Rodriguez A, Chang DT. Foreign body reaction to biomaterials. Semin Immunol 2008;20:86–100. https://doi.org/10.1016/j.smim.2007.11.004.

[43] Vergara-Irigaray M, Valle J, Merino N, Latasa C, García B, Mozos IR de los, et al. Relevant role of fibronectin-binding proteins in *Staphylococcus aureus* biofilm-associated foreign-body infections. Infect Immun 2009;77:3978–91. https://doi.org/10.1128/iai.00616-09.

[44] Zahariev M, Chen W, Visagie CM, Lévesque CA. Cluster oligonucleotide signatures for rapid identification by sequencing. BMC Bioinf 2018;19:395. https://doi.org/10.1186/s12859-018-2363-3.

[45] Klug A, Gramlich Y, Rudert M, Drees P, Hoffmann R, Weißenberger M, et al. The projected volume of primary and revision total knee arthroplasty will place an immense burden on future health care systems over the next 30 years. Knee Surg Sports Traumatol Arthrosc 2020:1–12. https://doi.org/10.1007/s00167-020-06154-7.

[46] Rosteius T, Jansen O, Fehmer T, Baecker H, Citak M, Schildhauer TA, et al. Evaluating the microbial pattern of periprosthetic joint infections of the hip and knee. J Med Microbiol 2018;67:1608–13. https://doi.org/10.1099/jmm.0.000835.

[47] Wildeman P, Tevell S, Eriksson C, Lagos AC, Söderquist B, Stenmark B. Genomic characterization and outcome of prosthetic joint infections caused by *Staphylococcus aureus*. Sci Rep-Uk 2020;10:5938. https://doi.org/10.1038/s41598-020-62751-z.

[48] Ma D, Brothers KM, Maher PL, Phillips NJ, Simonetti D, Pasculle AW, et al. *Staphylococcus aureus* genotype variation among and within periprosthetic joint infections. J Orthop Res 2021. https://doi.org/10.1002/jor.25031.

[49] McCarthy AJ, Lindsay JA. Genetic variation in *Staphylococcus aureus* surface and immune evasion genes is lineage associated: implications for vaccine design and host-pathogen interactions. BMC Microbiol 2010;10:173. https://doi.org/10.1186/1471-2180-10-173.

[50] Rasmussen G, Monecke S, Ehricht R, Söderquist B. Prevalence of clonal complexes and virulence genes among commensal and invasive *Staphylococcus aureus* isolates in Sweden. PLoS One 2013;8:e77477. https://doi.org/10.1371/journal.pone.0077477.

[51] Corrigan RM, Rigby D, Handley P, Foster TJ. The role of *Staphylococcus aureus* surface protein SasG in adherence and biofilm formation. Microbiology (Read) 2007;153:2435–46. https://doi.org/10.1099/mic.0.2007/006676-0.

[52] Geoghegan JA, Corrigan RM, Gruszka DT, Speziale P, O'Gara JP, Potts JR, et al. Role of surface protein SasG in biofilm formation by *Staphylococcus aureus*. J Bacteriol 2010;192:5663–73. https://doi.org/10.1128/jb.00628-10.

[53] Arciola C, Campoccia D, Gamberini S, Baldassarri L, Montanaro L. Prevalence of cna, fnbA and fnbB adhesin genes among *Staphylococcus aureus* isolates from orthopedic infections associated to different types of implant. FEMS Microbiol Lett 2005;246:81–6. https://doi.org/10.1016/j.femsle.2005.03.035.

[54] Young BC, Wu C-H, Gordon NC, Cole K, Price JR, Liu E, et al. Severe infections emerge from commensal bacteria by adaptive evolution. Elife 2017;6:e30637. https://doi.org/10.7554/elife.30637.

[55] Lower SK, Lamlertthon S, Casillas-Ituarte NN, Lins RD, Yongsunthon R, Taylor ES, et al. Polymorphisms in fibronectin binding protein A of *Staphylococcus aureus* are associated with infection of cardiovascular devices. Proc Natl Acad Sci USA 2011;108:18372–7. https://doi.org/10.1073/pnas.1109071108.

[56] Piroth L, Que Y-A, Widmer E, Panchaud A, Piu S, Entenza JM, et al. The fibrinogen- and fibronectin-binding domains of *Staphylococcus aureus* fibronectin-binding protein A synergistically promote endothelial invasion and experimental endocarditis. Infect Immun 2008;76:3824–31. https://doi.org/10.1128/iai.00405-08.

[57] Khademi SMH, Sazinas P, Jelsbak L. Within-host adaptation mediated by intergenic evolution in *Pseudomonas aeruginosa*. Genome Biol Evol 2019;11:1385–97. https://doi.org/10.1093/gbe/evz083.

[58] Blanka A, Düvel J, Dötsch A, Klinkert B, Abraham W-R, Kaever V, et al. Constitutive production of c-di-GMP is associated with mutations in a variant of *Pseudomonas aeruginosa* with altered membrane composition. Sci Signal 2015;8. https://doi.org/10.1126/scisignal.2005943. ra36–ra36.

[59] Cui Z, Li Y, Cheng S, Yang H, Lu J, Hu Z, et al. Mutations in the embC-embA intergenic region contribute to *Mycobacterium tuberculosis* resistance to ethambutol. Antimicrob Agents Chemother 2014;58:6837–43. https://doi.org/10.1128/aac.03285-14.

[60] Jenul C, Horswill AR. Regulation of *Staphylococcus aureus* Virulence. Gram-Positive Pathogens. Third Edition 2019. https://doi.org/10.1128/9781683670131.ch41.

[61] Johnson M, Cockayne A, Morrissey JA. Iron-regulated biofilm formation in *Staphylococcus aureus* newman requires *ica* and the secreted protein *emp*. Infect Immun 2008;76:1756–65. https://doi.org/10.1128/iai.01635-07.

[62] Chan P, Foster S. Role of SarA in virulence determinant production and environmental signal transduction in *Staphylococcus aureus*. J Bacteriol 1998;180:6232–41. https://doi.org/10.1128/JB.180.23.6232-6241.1998.

[63] Jenul C, Horswill AR. Regulation of *Staphylococcus aureus* virulence. Microbiol Spectr 2019;7:669–86. https://doi.org/10.1128/microbiolspec.gpp3-0031-2018.

[64] Clarke N, Loughman A, Meade G, Foster T. Molecular basis for *Staphylococcus aureus*-mediated platelet aggregate formation under arterial shear in vitro. Arterioscler Thromb Vasc Biol 2008;28:335–40.

[65] Merino N, Toledo-Arana A, Vergara-Irigaray M, Valle J, Solano C, Calvo E, et al. Protein A-mediated multicellular behavior in *Staphylococcus aureus*. J Bacteriol 2009;191:832–43. https://doi.org/10.1128/jb.01222-08.

[66] Viljoen A, Viela F, Mathelié-Guinlet M, Missiakas D, Pietrocola G, Speziale P, et al. *Staphylococcus aureus* vWF-binding protein triggers a strong interaction between

clumping factor A and host vWF. Commun Biology 2021;4:453. https://doi.org/10.1038/s42003-021-01986-6.

[67] Ko Y-P, Liang X, Smith CW, Degen JL, Höök M. Binding of efb from *Staphylococcus aureus* to fibrinogen blocks neutrophil adherence. J Biol Chem 2011;286:9865–74. https://doi.org/10.1074/jbc.m110.199687.

[68] Burch WMSR and RL, Burch Rl. The principles of humane experimental technique. vol. 1, 1959, https://doi.org/10.5694/j.1326-5377.1960.tb73127.x.